The X-J model: perovskite superconductors and heavy fermions

1992 J. Phys.: Condens. Matter 4 3235

(http://iopscience.iop.org/0953-8984/4/12/015)

J. Phys.: Condens. Matter 4 (1992) 3235–3260. Printed in the UK

The X–J model: perovskite superconductors and heavy fermions

M W Long
School Of Physics, Bath University, Claverton Down, Bath, BA2 7AY UK

Received 2 July 1990, in final form 25 January 1991

Abstract. The X–J model is a strong-coupling limit of both the natural tight binding model of perovskite superconductors and the Anderson lattice model of heavy fermions. The application of the model to perovskite superconductivity is straightforward, but its use to describe heavy fermions is more speculative. The straight-line motion of charge carriers in the model is sympathetic to antiferromagnetic correlations along the path traversed, although the motion destroys the long-range antiferromagnetic order by exchanging the two sublattices in passing. Antiferromagnetism is destroyed in both the square lattice geometry relevant to a CuO_2 plane and the triangular geometry relevant to an isolated layer of $CeAl_3$. A paramagnetic phase with shorter range correlations than suggested by the Heisenberg model seems preferred by the charge-carrier motion in these two-dimensional examples.

1. Introduction

The theoretical study of high-temperature superconductivity involves the analysis of charge carriers in systems with atoms which have lost almost all of their valence fluctuations. For most perovskite superconductors there is a parent compound which is an antiferromagnetic insulator. The moment resides on copper atoms in a CuO_2 layer which have an atomic Cu^{2+} configuration with one hole in their unfilled d-shells carrying spin-$\frac{1}{2}$. It is this copper atom which has lost almost all of its valence fluctuations, the only remnant being the superexchange interaction between nearest neighbours, probably involving virtual Cu^{+} excitations. Superconductivity is achieved by doping extra holes into the CuO_2 layer. It is believed that these extra holes reside dominantly on oxygen atoms and therefore that the copper atom valence is not significantly altered. The almost immediate loss of antiferromagnetism with hole doping suggests, however, that the charge motion is intimately coupled to the virtual copper valence fluctuations. Also, a comparison between NMR on copper and oxygen atoms suggests that the same excitation is being probed by NMR on either atom and hence that excitations are spread across both atoms. One model for this system presently under investigation is the t–J model [1], but we will study a similar but slightly different model; the X–J model [2].

A second collection of systems with atoms which have lost almost all their valence fluctuations are the heavy fermion systems [3]. For these systems the atom with restricted valence (called the 'special atom') is cerium (we will ignore uranium in this article) which has a single f-electron in a Ce^{3+} core. Again it is charge motion which is central to the theoretical analysis. The charge carriers near the Fermi

0953-8984/92/123235+26$04.50

surface become coupled to the cerium sites through virtual Ce^{4+} excitations and the materials exhibit quite bizarre properties. As well as the enormous effective masses, these materials do not exhibit the magnetism to be expected for rare earth compounds and, further, $CeCu_2Si_2$ is a superconductor with a remarkably small coherence length [4] by analogy with the perovskite superconductors. We believe that these systems should also be modelled by the X–J model which is a strong-coupling limit of the usual description; the Anderson lattice [5].

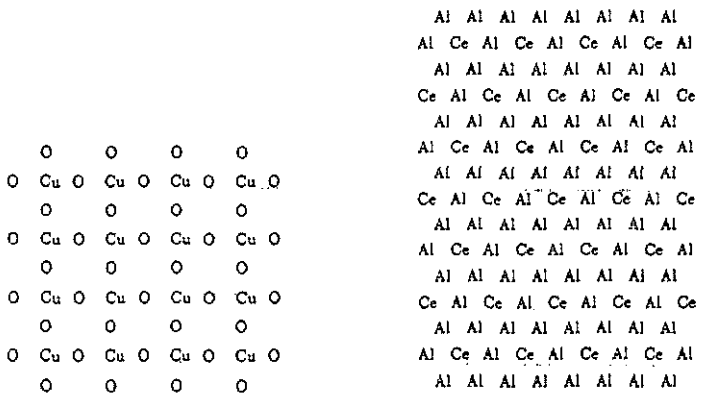

Figure 1. The square lattice geometry of a CuO_2 layer and the triangular lattice geometry of a $CeAl_3$ layer. The CuO_2 layers are fairly well insulated from each other but the $CeAl_3$ layers are strongly coupled.

We believe that the two planar geometries depicted in figure 1 are the basic geometries from which an understanding of CuO_2 and $CeAl_3$ can be deduced. The X–J model can be used to describe both systems, although for the CuO_2 system we describe holes whereas for $CeAl_3$ we describe electrons. Restricting attention to hybridization between atoms the X–J model is

$$H = X \sum_{\langle ij\rangle\sigma} \sum_{\langle ij'\rangle\sigma'} d^{\dagger}_{i\sigma} d_{i\sigma'} p^{\dagger}_{j'\sigma'} p_{j\sigma} e^{i(\phi_{ij}-\phi_{ij'})} + J \sum_{[ii']} \boldsymbol{S}_i \cdot \boldsymbol{S}_{i'} \qquad (1)$$

where $d^{\dagger}_{i\sigma}$ is an operator which creates a particle on the atom with restricted valence while $p^{\dagger}_{j\sigma}$ creates a particle on the surrounding atoms. The first term corresponds to the motion of the mobile charge carrier across a special atom by an intermediate valence fluctuation on that special atom. The second term corresponds to Heisenberg superexchange between two special atoms with $\boldsymbol{S}_i = \frac{1}{2}\sum_{\sigma\sigma'} d^{\dagger}_{i\sigma} \hat{\sigma}^{\sigma\sigma'} d_{i\sigma'}$ being a spin operator and $\hat{\sigma}$ being Pauli matrices. The phase factors ϕ_{ij} have been included in order to account for the angular variation of the relevant orbitals for the electrons on the special atoms. Both the d-orbitals and f-orbitals yield oscillations in phase, four nodes for the d-orbitals and six nodes for the f-orbitals. We are free to choose the relative phase between orbitals on different atoms in any way we like, but the choice around closed loops is *fixed* by the changes in phase encountered in circling the loop. For the bipartite geometry of the perovskite superconductors the phases may be consistently chosen to vanish. The choice for $CeAl_3$ is not so clear but is crucial as we will argue later.

Although for the perovskite superconductors the coherence between charge carriers is the most important problem, we will not address this issue but will study the

coherence amongst the spins on the special atoms instead. The magnetism, or lack of it, can be understood by a study of one charge carrier in interaction with the spin system, and it seems plausible that an understanding of one charge carrier is a prerequisite to the study of two. For $CeAl_3$ however, the reason for the paramagnetism of the spin system is a central issue.

In a recent publication it was pointed out that charge motion in the X–J model promotes *low-spin* correlations amongst the spins in the system [2]. This is contrary to the usual behaviour in strongly correlated systems. Nagaoka ferromagnetism is normally to be expected. A study of the linear chain was used to demonstrate the effect, but one important issue was left unresolved; what are the long-range properties of the spin correlations induced by the charge carrier? A cursory examination of [2] might suggest a broken symmetry for the ground state. In section 2 we address the question numerically and show that the charge motion induces essentially identical correlations to the Heisenberg interaction for the linear chain. In section 3 we present a simplistic description of $CeAl_3$ showing how to describe the system with the X–J model and how paramagnetism may well be preferred. Numerical results for the triangular and square lattices are presented in sections 3 and 4 respectively, and a simple analytic interpretation is supplied in section 5. In section 6 we conclude.

2. The X–J model on a linear chain

It was established in a recent article that charge-carrier motion in the X–J model prefers low-spin correlations [2]. In a search for more understanding of the model, we have performed a numerical investigation of the linear chain geometry of alternating special atoms and conduction atoms, in order to try to establish the character of the long-range spin correlations of the model, and hence to deduce the likely form of the low lying excitations; is the spectrum gapped?

We performed exact diagonalization studies on systems with up to 20 spins using the Lanczos algorithm. The convergence is poor with several hundred basis states required for a good description of the ground-state correlations; as is to be expected [6].

A finite-size scaling analysis of the ground-state energy for one charge carrier in the absence of Heisenberg interactions is depicted in figure 2. We find clear convergence to a value of $-2.887X$ which is within 1% of our previous analytic estimate based on a basis of only eight variational states [2].

The even-membered chains have an extra spin-$\frac{1}{2}$ which we assume forms a 'spinon' complicating the picture. As pointed out in our previous work [2], with periodic boundary conditions there is an alternation in ground-state energies as the length of an odd chain is increased. However when we consider *antiperiodic* boundary conditions we find the complementary states to those with periodic boundary conditions. For the even-membered chains depicted in figure 2, there are clearly two classes of states being scaled. The lower curve has spin-0 while the upper curve has spin-1. The surprise is that the states corresponding to a particular class correspond to *alternating* choices of boundary conditions. When we consider higher dimensional geometries, the spin correlations on particular loops that optimize particle motion will depend upon the local boundary conditions, which in turn are controlled by the topological phase factors ϕ_{ij}. Since for the upper class we require total spin-1 around the loop, strong paramagnetism is *only* predicted when the boundary conditions correspond to

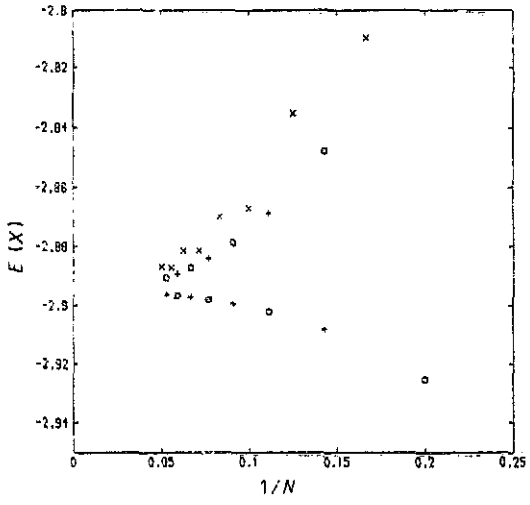

Figure 2. A finite-size scaling analysis of the ground-state energies of the X-model applied to the linear chain. The vertical and horizontal axes are energy (in units of X) and inverse chain length, respectively. Periodic boundary conditions are denoted by (o) for odd chains and (×) for even chains, and antiperiodic boundary conditions are denoted by (+) for odd chains. The odd chains have zone-centre or zone-boundary ground states whereas even chains have non-interacting Fermi surface momentum which can be attributed to the motion of the extra spin-$\frac{1}{2}$, often called a spinon.

the lower class. There is always the possibility of strong local paramagnetic correlations for any odd-membered loop; for loops of length 1 modulo 4 we require periodic boundary conditions while for loops of length 3 modulo 4 we require antiperiodic boundary conditions. Both possibilities can be physically significant as is pointed out in the next section. In our previous paper [2], we pointed out that the basic reason for this alternation in ground-state energy was associated with whether or not there was a resonant or cancelling superposition of the two states where all spins were paired into nearest-neighbour singlets. We will maintain this description.

We now move on to our study of the spin correlations induced by the charge-carrier motion. The ground state spin correlations in the *absence* of Heisenberg interactions can be readily understood in terms of a Heisenberg ground state! The comparison is complicated by the fact that one system has a charge carrier and the other does not. Further, the charge carrier is fully delocalized and the spin correlations depend on the behaviour of the charge carrier. For the ground state with the charge carrier delocalized, we have determined the *conditional* spin correlations subject to the charge carrier being found on a fixed atom and compared these with a system without any charge carriers. The conditional spin correlations for a certain chain are very similar to the Heisenberg ground-state correlations for a chain with one extra atom. The charge carrier itself has a spin and this spin participates in the spin correlations on an equal footing with the spins on the special atoms.

The X-model ground states with the resonant superposition are total spin-0 states whereas the X-model ground states with a cancelling superposition are total spin-1 states and must be compared with a Heisenberg state with one spin wave. The Heisenberg energies are compared in table 1, and there is clearly an enormous similarity and overlap between the two states. A comparison of the two types of correlations shows that the difference occurs in the near vicinity of the charge carrier, where the probability of finding the charge carrier in a relative spin singlet with its two neighbouring spins is enhanced.

These results may be readily understood in terms of an interpretation of the

Table 1. A comparison between the conditional Heisenberg energy of the ground state of the X-model and the energies of the ground states and some low lying excitations of the Heisenberg model. A chain of length N plus one charge carrier is compared with a Heisenberg chain of length $N+1$. The Heisenberg ground states are restricted to the subspace with identical total spin to the X-model ground state, and the excited state is the lowest lying state also with the same quantum numbers. The X-model ground state clearly almost simultaneously diagonalizes the Heisenberg model.

N	BCs	S	X-model ground-state energy	Heisenberg energy of X-model state	Heisenberg ground-state energy	Heisenberg excited-state energy
3	AP	0	−3.0000	−2.0000	−2.0000	0.0000
3	P	1	−2.5616	−0.8638	−1.0000	—
4	P	1/2	−2.6458	−1.7817	−1.8680	−0.7500
5	P	0	−2.9254	−2.7760	−2.8028	−1.5000
5	AP	1	−2.7913	−1.9361	−2.1180	—
6	P	1/2	−2.8095	−2.6781	−2.8552	−1.8062
7	AP	0	−2.9083	−3.6106	−3.6511	−2.6996
7	P	1	−2.8478	−2.9669	−3.1284	—
8	P	1/2	−2.8356	−3.7083	−3.7974	−2.9361
9	P	0	−2.9023	−4.4681	−4.5154	−3.7706
9	AP	1	−2.8689	−3.9511	−4.0922	—
10	P	1/2	−2.8673	−4.5940	−4.7190	−3.9920
11	AP	0	−2.8996	−5.3356	−5.3874	−4.7774
11	P	1	−2.8788	−4.9069	−5.0315	—
12	P	1/2	−2.8702	−5.5480	−5.6296	−5.0019
13	P	0	−2.8982	−6.2095	−6.2635	−5.7481
13	AP	1	−2.8842	−5.8424	−5.9564	—
14	P	1/2	−2.8816	−6.4314	−6.5337	−5.9818
15	AP	0	−2.8973	−7.0854	−7.1423	−6.6966
15	P	1	−2.8873	−6.7657	−6.8721	—
16	P	1/2	−2.8817	−7.3567	−7.4336	−6.9414
17	P	0	−2.8968	−7.9622	−8.0228	−7.6305
17	AP	1	−2.8894	−7.6820	−7.7815	—
18	P	1/2	−2.8872	−8.2410	−8.3305	−7.8865
19	AP	0	−2.8965	−8.8436	−8.9044	−8.0725
19	P	1	−2.8907	−8.5901	−8.6864	—
20	P	1/2	−2.8869	−9.1528	−9.2254	−8.8210

Hamiltonian. The X-model may be rearranged to form an exchange between the charge-carrier spin and its nearest-neighbour spins, combined with an exchange where the charge carrier simultaneously moves [7]. In the near vicinity of the charge there is a small enhancement of the singlet correlations making use of the static exchange where the charge carrier does not move, but the dominant long-range effect comes from motion along the chain which decides the more distant correlations. When the particle arrives it desires a high probability of being in a relative spin singlet with its two neighbours. By definition, the highest probability of finding *all* nearest-neighbour spins simultaneously in relative singlets is achieved by the ground state of the Heisenberg Hamiltonian, and far from the charge carrier this constitutes precisely the correlations found.

Although the ground state of the infinite Heisenberg chain has no long-range order, it does have power law decay of Néel correlations, and these correlations are strong enough to yield most of the properties to be expected of classical

antiferromagnetism; gapless spin-wave excitations and gapless spin spirals. We have compared conditional spin correlations under the assumption that the charge carrier is on a fixed atom, and in fact the charge carrier is fully delocalized. The motion of the charge carrier *destroys* the antiferromagnetic correlations.

An understanding of the spin correlations in the ground state is achieved through an analysis of the *conditional* spin correlations. Unfortunately these spin correlations are *not* those measured in most experiments, including neutron scattering. A neutron scatters off the spin density on the special atoms, but the relevant spin correlations are those *averaged* over the motion of the charge carriers; *unconditional* spin correlations. In order to understand the measured or 'actual' spin correlations on the special atoms, we must study the unconditional spin correlations between pairs of special atoms, averaged over the motion of the charge carrier. If we pick two special atoms, then the loop is cut into two segments. The relative orientation of the two spins on these atoms depends on the position of the charge carrier. On average the relative orientation of the two spins is in opposite directions when the charge carrier lies on one side of the loop compared with when it resides on the other side. The spin correlations are reduced by a factor reflecting the fraction of time that the charge carrier lies between the two relevant spins. Spins on opposite sides of the ring are decorrelated by the charge carrier, and only spins much closer together retain the antiferromagnetic correlations.

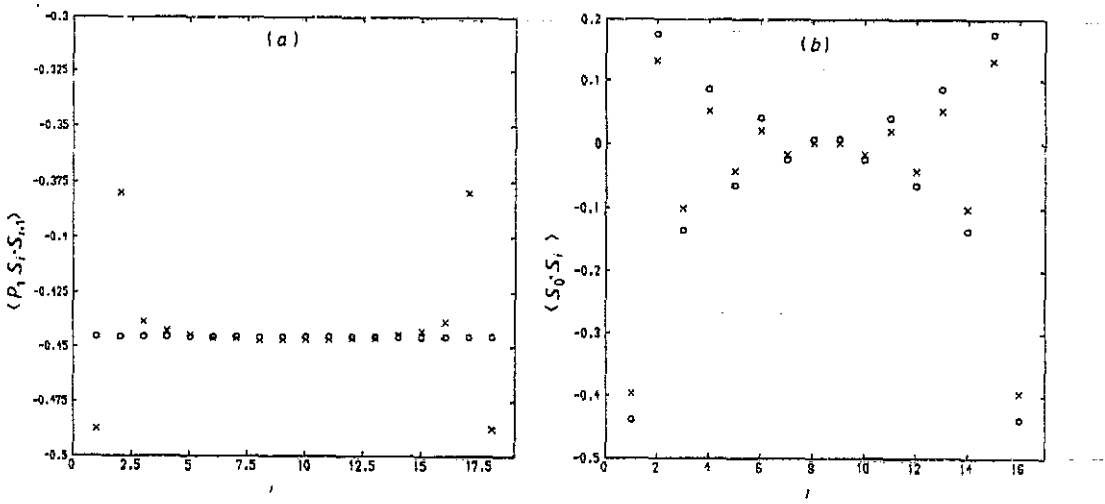

Figure 3. (*a*) Nearest-neighbour spin correlations conditional on the charge carrier being on a fixed atom versus distance away from the charge carrier. We have used a 17-atom chain with periodic boundary conditions, and the spin on the charge carrier is included as one of the spins. The two strongest singlet correlations involve the charge carrier, and the correlations for the ground state of the 18-atom Heisenberg chain, denoted by (o), have been plotted for comparison. (*b*) The actual spin correlations on the special atoms versus separation of the spins. The charge-carrier motion has been averaged over and has decorrelated the more distant spins. The spin correlations for the ground state of a 17-atom Heisenberg chain, depicted by (o), have been plotted for comparison.

In figure 3 we depict a selection of spin correlations for a system of 17 atoms. The conditional spin correlations are seen to be very similar to those for the Heisenberg chain of eighteen atoms. The *actual* spin correlations averaged over the charge-carrier position die out quite quickly, but strangely they do resemble the correlations of a

Heisenberg chain of 17 atoms. For an odd-membered Heisenberg chain the total spin must be at least a half. This excess spin may be considered as a spinon; a type of chargeless quasiparticle [8]. It is this spinon which decorrelates the spins on an odd-membered Heisenberg chain in an analogous way to the way the charge carrier decorrelated the spins in the X-model. The natural interpretation then suggests that the spinon found when studying the strongly correlated atoms alone, is paired up with the spin on the charge carrier. The additional charge carrier has separated into a spinon, which has paired up with the spinon associated with the odd-membered chain, leaving a spin-0 charged particle or holon.

A more thorough understanding of this spinon and holon picture can be achieved using the 'domain wall' interpretation of spin-$\frac{1}{2}$ Heisenberg interactions [8]. For a Heisenberg chain with an odd number of atoms a Néel state *requires* a pair of neighbouring parallel spins; a domain wall. The spinon is a delocalized domain wall. When we analyse our X-model ground state, the two special atom spins neighbouring the charge carrier are almost always parallel in the ground state. The domain wall in the 17-atom loop is located at the charge carrier. As the charge carrier moves around, so the domain wall moves with it, being bound to it.

We have performed analogous numerical calculations to those so far presented for the case of two charge carriers. Once again an understanding is achieved through the study of conditional spin correlations. The details will be presented at a later date, but the physics is transparent. The ground state is *still* controlled by Heisenberg correlations. The two spins on the charge carriers become included in an augmented chain which has an almost precise Heisenberg ground state. The charge carriers delocalize and weakly repel each other. The repulsion is somewhere between that found in spinless fermions and non-interacting bosons.

For the infinite chain with a finite density of charge carriers, the Heisenberg correlations for the augmented chain, with charge carrier spins included, will remain. The charge carriers will delocalize and weakly repel, but compared with spinless fermions they will be *attracted* to each other. Although the conditional spin correlations will be Heisenberg correlations, the actual spin correlations restricted to the special atoms do not extend far. Each charge carrier includes a spinon into the special atom chain. The actual antiferromagnetic-spin correlations only extend as far as the average distance between two charge carriers.

Although the actual spin correlations are quickly destroyed by the charge-carrier motion, this does not mean that the Heisenberg energy is small. Indeed the actual Heisenberg energy is quite close to the optimum value in the absence of the charge carriers. The reason is simple: the Heisenberg contribution does not affect the charge carrier and so the states on which the Heisenberg interaction acts are those corresponding to the *conditional* spin correlations, and these correlations are locally very nearly the Heisenberg ground state.

The X-model charge motion very nearly simultaneously diagonalizes the Heisenberg interaction on the linear chain, although the long-range element to the antiferromagnetic correlations is severely curtailed and will be destroyed at very low doping concentrations. This is absolutely opposite behaviour to the much studied t–J model. For the t–J model there is a fierce competition, with the *local* correlations being energetically in opposition.

The excitations found in the X-model are not well represented by the Heisenberg excitations. The motional energy is only weakly affected by distorting spins far from the charge carrier although the Heisenberg energy is severely modified. A lot more

effort is required in order to achieve some interpretation for the excitations.

The physical systems are higher dimensional and are expected to exhibit rather different behaviour. The closed topological loops break the degeneracy of the short-range spin correlations and stabilize the local-spin correlations suggested by the relevant small-loop calculations of this section. A charge carrier now finds many possible paths open to it and there is a competition between all the possible paths and their preferred correlations. The spin on the charge carrier *still* becomes involved in the spin state of the special atom system and the charge carrier itself delocalizes independently: the spin and charge degrees of freedom still separate. In two dimensions a special atom has more than two nearest neighbours. When a charge carrier performs motion along a path which passes across a particular special atom, the path usually involves only *two* nearest neighbours. The spins along that path will exchange sublattices and this will break down the correlations between the particular special atom and the nearest neighbours which are *not* traversed by the charge carrier. The Heisenberg spin correlations can be broken down completely by charge-carrier motion which can induce quite different correlations at long distances. We believe that only short-range spin correlations survive.

In the next two sections we will investigate the correlations induced in our two-dimensional planar examples numerically.

3. A planar model for $CeAl_3$

3.1. Applying the model to $CeAl_3$

There are several important physical complications which are encountered in attempting to describe $CeAl_3$ with the X–J model.

The first and most important problem is the assumed dominance of the hybridization across aluminium atoms. The usual description for heavy fermion materials is the Anderson lattice [5]. The dominant hybridization is assumed to be between the conduction states with only a weak hybridization between the special atoms and the conduction states. The X–J model is the strong-coupling limit of the Anderson lattice for a rather different parameterization; when the conduction electron hybridization is negligible [9].

The second natural problem is spin–orbit coupling. Most rare earth atoms exhibit atomic physics properties even in the solid state, with the atom exhibiting only some values of the total angular momentum at low temperatures. Experimentally spin–orbit splitting can be easily measured with inelastic neutron scattering [10], and for $CeAl_3$ it has been established that at the relevant temperatures the spin–orbit splitting is effectively complete with a well defined $J = \frac{5}{2}$ ground state and a $J = \frac{7}{2}$ spin–orbit level at about 250 meV [10]. The X–J model has spin decoupled from the orbital angular momentum, and whether or not this simplification is sensible must be determined.

The third physical problem is with the model itself. For bipartite lattices the loops have even numbers of atoms which, with the charged particle itself, ensures an odd number of spins around a closed path and none of the resonant effects associated with the odd loops. For the perovskite superconductors we find quantum paramagnetism as hoped and as will be discussed in the next section. For the geometry of figure 1 we find triangles which are the *worst* choice for paramagnetism with the resonant contribution vigorously disfavouring low spin and preferring ferromagnetic coupling.

The resolution of these three physical problems are interelated and constitute our modelling of the material.

The relevant electronic degrees of freedom on the aluminium atoms are s- and p-orbitals. As a first pass, let us ignore the p-orbitals and study the s-orbitals alone. The aluminium atoms form a Kagome net†, and the band structure for nearest-neighbour hopping on the Kagome net is $\epsilon(\gamma_k)$:

$$\epsilon(\gamma) = 2t \qquad -t \pm \sqrt{[3(1+2\gamma)]}t \tag{2}$$

which is depicted in figure 4, in terms of γ_k the structure factor for the cerium triangular lattice. The interesting feature is the flat band at the top of the figure. In figure 5 we depict the phases of a localized state which forms this flat band. It can be orthonormalized to form a Wannier orbital if desired, in an analogous way to the treatment of the bonding combination of oxygen states in a CuO_2 plane [11]. In the real materials this band would gain dispersion from the effects that we have so far ignored.

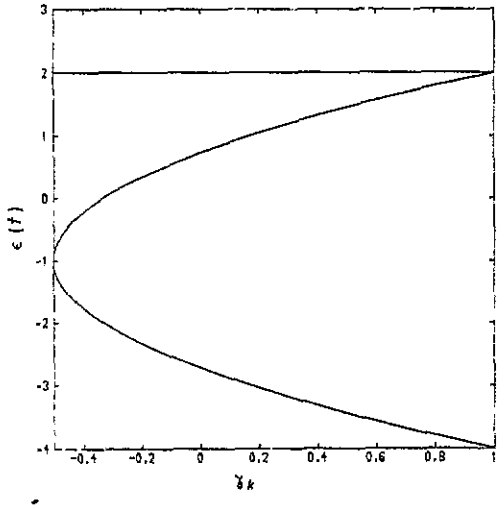

Figure 4. The dispersion of a single tight binding s-orbital on a Kagome net. The vertical and horizontal axes are energy in units of the hopping matrix element and triangular lattice structure factor, respectively. The important feature is the flat band at the top of the spectrum.

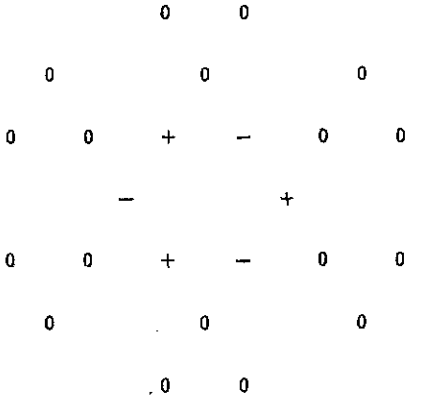

Figure 5. A localized wavefunction which gives rise to the flat band of figure 4.

It is clear that the s–p hybridization will allow dispersion from nearest-neighbour hopping in the plane, next nearest-neighbour matrix elements will allow dispersion in the plane, and hopping to neighbouring layers will also induce dispersion. The possibility that we would like to consider is that the *dominant* process is delocalization onto the cerium atoms. If this hybridization is to dominate these other effects, then it cannot be very small, and we must develop a new explanation for the reason why the charged particles are so heavy.

† We believe that 'Kagome net' is the correct terminology.

Under the present assumptions we have a dispersionless 'conduction s-band' on the aluminium atoms which has perfect symmetry to hybridize with a $\hat{x}(\hat{x}^2 - 3\hat{y}^2)$ or $\sin^3\theta\cos 3\phi$ f-electron on the cerium atom. Assuming that Ce^{2+} is energetically inaccessible and that the dominant delocalization process is via intermediate virtual Ce^{4+} excitations, then we are led to the X–J model; equation (1) for *the motion* of charge carriers on the aluminium atoms and superexchange across the aluminium atoms [9].

For the assignment $Ce^{3+}Al_3^-$, each aluminium atom would have four valence electrons and then any s-electrons above four-thirds per aluminium atom might be expected to be described by this model. We would naively guess that only a low concentration of electrons would be involved.

If we take the present derivation at face value, then we are led to a resolution of the problem that triangles do *not* promote low-spin correlations, the physical requirement of the model. When we focus on a single triangle present in the geometry, an analysis of which of our one-dimensional loop calculations is analogous yields a surprise. We discover that the motion involves *antiperiodic* boundary conditions around the triangle. *There is a topological phase shift* around a triangle. The phases, ϕ_{ij}, conspire to enforce an extra change in phase for motion around each triangle. Hopping once around a triangle involves three changes of sign, at each cerium atom, and this converts the usual resonant cancellation preferring spin-1 into a superposition preferring spin-0, and this locally stabilizes the low-spin correlations, as we shall soon show.

Our first task is to establish the energy scale on which the aluminium electrons become 'bound' to the f-electrons. This is the energy scale which must dominate the 'free-electron' delocalization processes which are being ignored.

If we consider a single cerium atom with one electron delocalized by the X–J model on the six surrounding aluminium atoms, then the ground state finds the aluminium and cerium electrons in a relative spin singlet at an energy of $-6X$, with the nearest excited state at zero energy. Although the energy scale X may be relatively small, the local 'Kondo' singlet is stabilized by an extra factor of the coordination number in this case six, which is always very large in heavy fermion systems. We believe that it is this large coordination number which stabilizes the heavy fermion state and *not* the large f-degeneracy as has previously been argued [5]. The f-degeneracy of the cerium atom is removed on a much larger energy scale than that on which the heavy fermion coherence and even the Kondo coherence are relevant. The atom is almost always effectively a doublet.

In the Kondo effect, a conduction electron close to the Fermi surface becomes trapped in a relative spin singlet with an isolated localized moment. The energy gain stabilizing this state is the hybridization *between* the localized electron and the conduction states. A single aluminium electron in a relative spin singlet with a cerium electron is conceptually analogous, and plays the role of the 'Kondo' singlet in our model. The main difference between the two models is that the Kondo singlet in this article is short-ranged in real space. The reason for this requirement is elementary, the conduction electron hybridizes with the *nearest* local moments, and so singlet correlations beyond nearest neighbours are pointless. If the conduction electron is mobile and moves across several unit cells between interactions with local moments, then the description that results is free electrons combined with an RKKY interaction between local moments. The consequence is magnetism. *We must avoid this scenario at any cost.*

Our resolution to this problem is to allow the hybridization between the localized

electrons and the conduction electrons to *dominate*. The relevant energy is *very* small and so domination will be rare: heavy fermion behaviour *is* rare. For the present model the Kondo singlet is stabilized on the energy scale of ZX, where Z is the coordination number between a special atom and its nearest-neighbour conduction atoms. It is clear that our desription is most likely to apply when the coordination number is large: heavy fermions always have a large coordination number (indeed for UBe_{13}, $Z = 24$!). We believe that the X-model is the most likely limit of the Anderson lattice in which to expect heavy fermion behaviour. The real justification for the model is in demonstrating that the behaviour that it predicts is precisely that found in heavy fermion systems. In this article we will show that the preferred spin coherence is very short-ranged paramagnetism in basic agreement with the experimental systems. We will also show that spin–charge separation is quite natural, although the final consequence, that the charge carriers are almost non-interacting, bosonic and very heavy, is left to the future.

At this point we should point out that the model finds the two particles exchanging spins very frequently while the orbital angular momentum is assumed fixed. The spin–orbit coupling is therefore not being favoured and we are assuming that the hybridization energy of $-6X$ is dominating the spin–orbit coupling and stabilizing the local 'Kondo' singlet. Although this might be the case in some materials, it is clearly not true in $CeAl_3$ which has well defined spin–orbit levels. The resolution to this contradiction is to assume that in fact the f-electrons actually reside in states with fixed J_z, i.e. slight modifications to $\exp(+i3\phi)\,|\downarrow\rangle$ and $\exp(-i3\phi)\,|\uparrow\rangle$, and suffer a reduced hopping rate into the orbitals with the relevant $\cos(3\phi)$ symmetry. We would expect a simple reduction by a factor of about two in the matrix element X, but no real change in the form of the model. The fact that the spin–orbit splitting dominates does place an upper bound on the energy involved in the coupling which must be less than $\sim \frac{1}{4}$ eV.

The next important task is to try to understand the spin correlations amongst the surrounding cerium spins which allow delocalization of the electron on the aluminium atoms. It is the strong stabilization of local paramagnetic correlations which has motivated our study of the X–J model and the natural behaviour that it exhibits. Although it is clear that the X–J model is an oversimplification, the model does involve strong coupling between charge-carrier motion and the spin system, and we hope that it exhibits behaviour of some relevance to heavy fermion systems.

3.2. Numerical simulations of the X–J model

The results of section 2 provide the behaviour to be expected. The smallest loop is a triangle and the local phase relationship from circling the loop is equivalent to anti-periodic boundary conditions. This is a critical result in deciding the resulting spin coherence: when an electron circuits a loop, it picks up *three* phases, i.e. $\phi_{ij} - \phi_{ij'} = \pi$, from the f-orbitals on the cerium sites. This leads to *antiperiodic* boundary conditions for locally circling a triangle. If this argument had yielded local periodic boundary conditions, then the resulting spin coherence would have been *ferromagnetic*, in agreement with Nagaoka and RKKY, and in direct contrast to the desired result. The motional energy for the charge carrier is optimized on a triangle when the three spins on the cerium atoms and the spin on the aluminium electron are found in a total spin singlet; *low-spin correlations are preferred*. The energy gap to the lowest lying excitation is large being of order X so low spin is stabilized quite strongly.

The transition from one to two dimensions involves some new phenomena. In the absence of double occupancy of oxygen atoms, the spin degeneracy of the copper chain remains unbroken for the infinite chain. Whatever the spin configuration the charged particle can only hop to its two neighbouring sites and these hops can be optimized independent of the spin configuration. In two dimensions we have small topological loops together with a multiplicity of connections for the atoms surrounding a special atom.

If we consider all the atoms which surround one special atom, then a charge carrier on any atom can hop to any other atom across the special atom. This is the highest degree of connectivity possible and produces the strongest topological effects. For the present case it leads to the stabilization of the local spin singlet on the ZX energy scale, where Z is the coordination number of the special atom.

The next consideration is topological loops and it is motion around loops which tends to decide the spin coherence amongst the special atoms at a slightly greater distance from the charge carrier. For the present case we find antiperiodic boundary conditions around triangles which suggests low-spin correlations. It is important to appreciate that the stability of the local singlet does not guarantee paramagnetism. A study of periodic boundary conditions on the present lattice suggests that ferromagnetism is preferred far from the charge carrier, as is usual in the corresponding problem for the Hubbard model [12]. The p-orbitals which couple directly to the f-electrons would each supply an additional phase as a triangle is circled, which would convert the local boundary conditions *back* to periodic boundary conditions around a triangle suggesting local ferromagnetism, although the relevant states are unlikely to be close to the chemical potential.

We have studied the case with local periodic boundary conditions in some detail. Indeed, a closed form equation for the ground-state energy of the single-charge carrier problem is given in equation (4). The corresponding state is rather more subtle than that predicted by the Nagaoka problem. The Kondo interaction forces the existence of a Kondo singlet. However, the singlet is tightly bound to the charge carrier and the *composite* object delocalizes best in a ferromagnetic background.

The basic phenomena at work are straightforward but the correlations which result are not clear at all. Even the quantum mechanical Heisenberg model is as yet unsolved. For bipartite lattices long-range Néel antiferromagnetism is believed to result, although with a much reduced moment from the classical solution. The present lattice is an antiferromagnetically frustrated topology, and it is now known that for some such lattices the classical ground state is destabilized and replaced by quantum paramagnetism [13]. Indeed this is a possible explanation for the lack of antiferromagnetic order in $CeAl_3$. The classical solution for the Heisenberg model on the triangular lattice yields non-collinear antiferromagnetism with three sublattices, all nearest neighbours at 120° and all next-nearest neighbours parallel. This type of order is relatively easy to find if present.

The charge motion prefers local 'Kondo' singlet formation and delocalizes best on a paramagnetic background. The key issue to resolve is the *type* of paramagnetism which is locally preferred. In order to try to address this problem we have numerically investigated some small clusters with periodic boundary conditions. We have restricted attention to *odd* numbers of special atoms in order to allow total spin-0 solutions and no necessity for a 'spinon'. The ground state has zone-centre phase coherence and a low total spin.

The exponential growth of the number of degrees of freedom with system size

means that we are restricted to very small clusters. The use of periodic boundary conditions includes additional loops into the connectivity which can dominate in tiny clusters introducing anomalous behaviour. The cluster size to which we are restricted is still being severely modified by these additional loops, which must be included in any interpretation.

Our calculations on the linear chain indicate that even at this level we might discover the important effects. The secrets of the linear chain were uncovered by a study of the *conditional* spin correlations. The spin correlations were Heisenberg-like, with a modification in the vicinity of the charge carrier to enhance the probability that it is in a singlet with its two neighbouring spins. This enhancement takes place at the expence of the nearest-neighbouring pair of spins.

A typical collection of nearest-neighbour ground-state conditional spin correlations are depicted in figure 6. The spin correlations on the ten special atoms around the charge carrier are common to all the clusters for which the atoms are independent. The low-spin correlations far from the charge carrier are strongly dependent on the boundary conditions and do not involve much energy, being severely modified in the excited states which are only about 1% higher in energy at this order.

These spin correlations are easy to interpret: first there is the enhancement of the singlet character of the charge carrier with its nearest-neighbour spins that we found for the linear chain. Second, the resonant contribution from the charge carrier circuiting one of the two triangles on which it is located ensures that the singlet probability around these two triangles is enhanced in comparison with the other possible routes that the charge carrier can traverse. The singlet probabilities for pairs of spins next to the charge carrier are reduced in order to compensate for the enhancement at the charge carrier. Finally, the spin correlations on the eight atoms surrounding the charge carrier and its two neighbours have high singlet probability in order that the charge carrier has a high probability of arriving in a singlet with its neighbours when it arrives.

When we try to analyse the absolute correlation functions we encounter several interpretational difficulties. First, for most clusters, the boundary conditions break the point group symmetry yielding preferential directions for motion. The spin correlations vary quite dramatically in different directions and averaging over the point group appears to be the only way to extract results for comparison with the infinite system. Second, for most clusters, pairs of atoms fulfil several roles, being simultaneously next-nearest and third-nearest neighbours to the same atom for example. Third, the small size of clusters restricts attention to only about third-nearest neighbours, and very little can be deduced about the infinite system from such results. Accepting the complications, the results suggest that the nearest-neighbour correlations achieve a substantial fraction of the ground-state Heisenberg bond energy and that the more distant correlations are small. Some selected results are presented in table 2. There is no evidence whatsoever for classical antiferromagnetism which would show up as triplet correlations amongst next-nearest neighbours.

The underlying lattice for these calculations is the triangular lattice. The topological frustration strongly weakens the energy gain from classical ordering and it is not clear whether the ground state has long-range magnetic order. The present results are consistent with a 'resonating valence bond' [8] state being preferred by charge motion. We will attempt some plausible analytic interpretations in section 5.

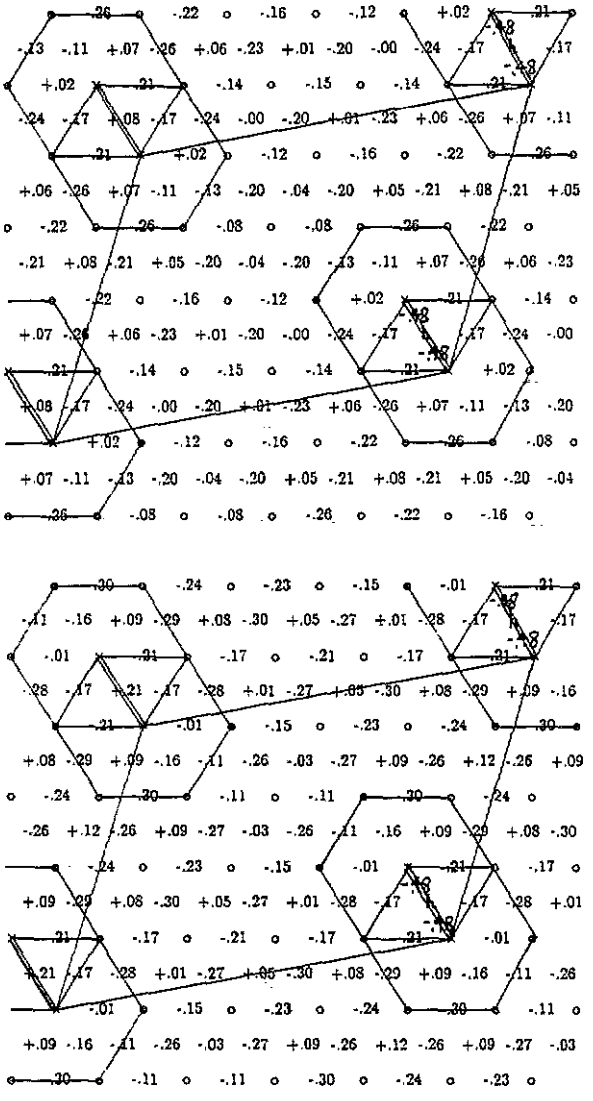

Figure 6. Nearest-neighbour spin correlations conditional on the charge carrier being fixed between the two starred atoms. There are 17 atoms with periodic boundary conditions. The top state is the spin-1 ground state at energy $-8.0234X$ and the lower state is the lowest lying spin-0 state at energy $-8.0214X$. The 10 atoms surrounding the charge carrier have similar correlations to those found in *all* our calculations. The connectivity induced by our periodicity clearly promotes motion in four of the six possible directions, which is not expected for the infinite system, and varies from cluster to cluster.

4. The perovskite superconductors

The derivation of the model for this case is now well established [14], and so we will only discuss our numerical study. Bipartite lattices have no odd loops and so the resonant effects are very small in comparison to those for the triangular lattice. The complications from the loops included in our periodic boundary conditions are much more important for this case since any odd paths included can easily dominate. We

Table 2. A selection of calculations on triangular lattice clusters with periodic boundary conditions on the edges, but varying boundary conditions around triangles. When ground states are degenerate we did not always calculate the correlations. The ground state is almost unaffected by the inclusion of strong-coupling interactions on the conduction atoms, whereas in one dimension the inclusion breaks the degeneracy. Antiperiodic boundary conditions lead to a low-spin ground state at energy $\sim -8X$ (or $\sim -7.2X$ when the conduction atoms are strong coupling). Periodic boundary conditions find one magnon bound to the charge carrier and all the other spins parallel in a ferromagnetic ground state at energy $\sim -8.2X$.

N	BCs	S	U_p	X-model ground-state energy	First nearest-neighbour correlation	Second nearest-neighbour correlation	Third nearest-neighbour correlation
3	AP	0	0	−9.0000	−0.2500	—	—
5	AP	1	0	−7.9330	−0.0831	—	—
5	AP	0	0	−7.5414	−0.1336	—	—
7	AP	0,1	0	−7.0000	−0.1071	−0.1071	—
9	AP	0,1,3	0	−7.8655	—	—	—
11	AP	0	0	−7.7608	−0.0878	−0.0366	−0.0525
13	AP	0	0	−7.9864	−0.1049	−0.0104	−0.0104
15	AP	0	0	−8.0705	−0.1440	+0.0067	+0.0673
17	AP	1	0	−8.0234	−0.1157	+0.0145	−0.0012
17	AP	0	0	−8.0214	−0.1362	−0.0034	+0.0258
3	AP	0	∞	−8.0000	−0.2500	—	—
5	AP	1	∞	−7.1241	−0.0890	—	—
5	AP	0	∞	−6.7876	−0.1384	—	—
7	AP	0	∞	−6.3723	−0.1072	−0.1072	—
7	AP	1	∞	−6.3687	−0.0610	−0.0610	—
9	AP	3	∞	−7.0545	+0.0442	+0.1910	+0.0442
9	AP	1	∞	−6.9976	−0.1392	+0.1943	−0.1392
9	AP	0	∞	−6.9708	−0.1764	+0.1959	−0.1764
11	AP	0	∞	−6.9666	−0.0863	−0.0379	−0.0528
13	AP	0	∞	−7.1307	−0.1033	−0.0121	−0.0121
15	AP	0	∞	−7.1990	−0.1438	+0.0088	+0.0667
17	AP	1	∞	−7.1688	−0.1148	+0.0123	−0.0004
17	AP	0	∞	−7.1638	−0.1345	−0.0042	+0.0278
3	P	1	0	−7.6847	—	—	—
5	P	2	0	−8.0664	+0.1550	—	—
7	P	3	0	−8.2621	+0.1797	+0.1797	—
9	P	4	0	−8.2222	+0.1966	+0.1928	+0.1966
11	P	6	0	−8.2291	+0.2060	+0.2049	+0.2050
13	P	6	0	−8.2104	+0.2131	+0.2116	+0.2116
15	P	7	0	−8.2115	+0.2181	+0.2167	+0.2168
17	P	8	0	−8.2131	+0.2217	+0.2207	+0.2209

have two choices; first we can accept the boundary condition complications and hope that the system size is adequate. Second we can use bipartite boundary conditions and tackle their associated problems. We have tried both options. Selected results are presented in table 3.

There are two complications associated with the choice of bipartite boundary conditions; first we require an even number of atoms, and with the addition of the charge-carrier spin this necessitates a spinon. Second this spinon tends to have a

Table 3. A selection of calculations on square lattice clusters with periodic boundary conditions. Daggered states have a Fermi surface wavevector and all others have a zone-centre wavevector. The ground state has low spin. The single bound magnon state has energy $-5.324X$ and so the low-spin state is only stable by $\sim X/5$.

N	S	U_p	X-model ground state energy	First nearest neighbour correlation	Second nearest neighbour correlation	Third nearest neighbour correlation
5	2	0	−5.4244	+0.1529	—	—
5	0	0	−4.4244	−0.1500	—	—
7	3	0	−5.3779	+0.1836	+0.1797	—
7	1	0	−5.3027	−0.0462	−0.0498	—
7	0	0	−5.0292	−0.1673	−0.0703	—
9	0	0	−5.5190	−0.2484	+0.0037	−0.2484
11	0	0	−5.4317	−0.0989	−0.0231	−0.0130
13	0	0	−5.4396	−0.0832	−0.0158	−0.0740
15	0	0	−5.5039	−0.2320	+0.0733	+0.0053
15	1	0	−5.4824	−0.1334	+0.0110	−0.0184
5	2	∞	−4.6056	+0.1320	—	—
5	0	∞	−3.7283	−0.1500	—	—
7	3	∞	−4.5529	+0.1673	+0.1676	—
7	1	∞	−4.4748	−0.1130	−0.1109	—
7	0	∞	−4.2277	−0.1701	−0.0697	—
9	0	∞	−4.5765	−0.1674	+0.0007	−0.1674
11	0	∞	−4.5793	−0.0987	−0.0191	−0.0145
13	0	∞	−4.5812	−0.0450	+0.0275	−0.0457
15	1	∞	−4.6155	−0.1293	+0.0086	−0.0204
15	0	∞	−4.6122	−0.2261	+0.0687	+0.0017
8	5/2	0	−5.2961†	+0.0595	+0.0976	+0.0097
8	7/2	0	−5.2915	+0.1993	+0.1824	+0.1824
8	3/2	0	−5.1955†	+0.0109	−0.1095	−0.0110
8	3/2	0	−5.1955	+0.0109	−0.2081	+0.1861
16	5/2	0	−5.3716†	−0.1007	+0.0414	−0.0052
16	7/2	0	−5.3689	−0.0373	+0.0382	+0.0383
16	3/2	0	−5.3675	−0.1295	+0.0391	−0.0791
16	1/2	0	−5.3663†	−0.1206	−0.0090	−0.1043
8	5/2	∞	−4.4509†	+0.0436	+0.1005	+0.0227
8	7/2	∞	−4.4051	+0.1915	+0.1720	+0.1720
8	3/2	∞	−4.3819†	−0.0007	−0.0982	−0.0053
8	3/2	∞	−4.3819	−0.0007	−0.1910	+0.1805
16	5/2	∞	−4.5319†	−0.1043	+0.0447	+0.0094
16	3/2	∞	−4.5220	−0.1033	−0.0694	+0.1056
16	1/2	∞	−4.5172†	−0.1186	+0.0052	−0.0999

wavevector associated with the non-interacting Fermi surface. The degeneracy of the Fermi surface is high, and analogous to the effects involved in Hund's rules of atomic physics, the degeneracy is lifted by exchange, which promotes ferromagnetism. Even though the charge motion promotes low-spin correlations, there is a non-trivial number of spinons in the ground state which confuses our interpretation of the cluster calculations. This Fermi surface degeneracy is not relevant for the infinite system, since as the system size increases, this moment scales only with the length of the

Fermi surface and this is macroscopically irrelevant. The behaviour of the spins close to the charge carrier is similar to that for the non-bipartite boundary conditions, although the wavevector of the state leads to a preferred direction of motion.

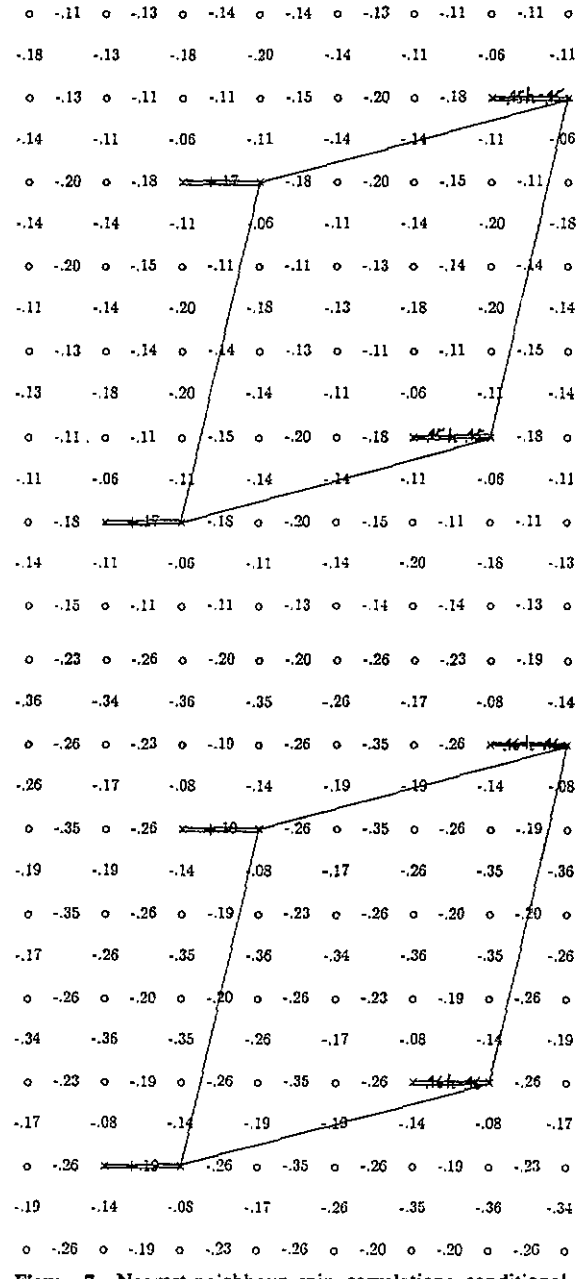

Figure 7. Nearest-neighbour spin correlations conditional on the charge carrier being fixed between the two starred atoms. There are 15 atoms with periodic boundary conditions. The conduction atoms are also assumed strong coupling for this case. The top state is the spin-1 ground state at energy $-4.6155X$ and the lower state is the lowest lying spin-0 state at energy $-4.6122X$. The correlations are quite typical. The second state has a fair quantity of Néel correlations.

A typical collection of conditional spin correlations are presented in figure 7. The interpretation is perfectly analogous to that for the triangular lattice. The singlet correlations between the charge carrier and its nearest neighbours are enhanced at the expence of the neighbouring correlations. The more distant correlations are strongly singlet in order that the charge carrier is more likely to arrive in a singlet as it moves about the lattice.

5. Analytic interpretations

In this section we make an attempt at introducing an interpretation for the results that we have found. In no way should one view this section as being the *actual* solution, but by analogy with the way that the classical Néel state describes the *physics* of the quantum antiferromagnet, we believe that the states suggested in this section will yield the physics and even the actual solution after a few 'quantum fluctuations' are included.

As has previously been discussed, the *non*-bipartite system is easier to understand in the vicinity of the charge carrier, because the inclusion of the spin degree of freedom on the charge carrier increases the effective length of the loops on which it sits by one, converting them locally into bipartite loops. The triangles of section 3 are increased locally into squares. A local Néel ordering on the resulting square then fully optimizes the charge motion around the triangle.

The key complication for the two-dimensional systems is the multitude of different paths that the charge carrier can take and the resulting differences between the spin correlations which result. Which paths are the preferred paths? Although there are many routes open to the particle, the ground-state energy indicates that only a certain fraction are used. An electron on an aluminium atom neighbours two cerium atoms. The electron can hop across each cerium to the six aluminium atoms which neighbour that cerium atom. This yields *twelve* possible hops in all. The numerical calculations show that the ground-state energy is approximately $-8X$, and so *one-third* of the possible hops do not lead to coherent motion and are avoided by the electron. In this section we attempt to understand which paths the electron chooses, and the role of the spin correlations in that choice.

The basic idea can be grasped with a study of a single cerium atom and its six neighbouring aluminium atoms. The spectrum for an electron moving with the X-model on this geometry finds a singlet ground state at $-6X$, but the nearest excited state is at *zero energy*. *Any* local triplet configurations *necessitate* a huge loss in energy and lead to highly excited configurations. Further, the zero-energy excitations involve *non-bonding* combinations which are *not* free to delocalize. The key to the X-model is to ensure that delocalization is into Kondo singlets, *as far as is possible*. We will present states composed of *precisely* the correct spin correlations to ensure this.

The states that we would like to propose as an interpretational aid, are those where the charge carrier is in a spin singlet with one of its nearest-neighbour spins and all the remaining spins are paired up in nearest-neighbour singlets. The Hamiltonian connects each such state to *seven* other such states directly. There are six matrix elements across the spin with which it is singlet correlated, together with one hop across the other nearest-neighbour spin in the direction of the spin which happens to be paired up with that spin. The connectivity and topological phases conspire to ensure that *all* seven of these hops can simultaneously contribute *in phase* if the

relative phases of a superposition of all the different spin configurations is chosen correctly. The resulting estimate of $-7X$ is quite close to the numerical bound which appears to be around $-8X$. The state comprising of an *equal* superposition of *all* the spin configurations with nearest-neighbour singlet pairs that a single charge carrier can get the spin background into with negative phase hops, is the state from which we believe that the physical insight into the *true* solution can be deduced.

In order to try to justify the use of the proposed wavefunction, we should first look at the five hops which have hitherto been neglected. All the neglected hops lead directly to spin configurations with singlets of longer range than nearest neighbours, but it is important to realize that the valence bond description so far described involves an important complication; *non-orthogonality*. Different valence bond spin configurations have non-trivial overlaps and can be simultaneously describing the same physics, which complicates matters. The seven hops so far discussed are unaffected by the non-orthogonality problems since each state is produced precisely seven times in an application of the Hamiltonian and so provided the superposition does not vanish we find an energy of $-7X$ from these hops. Although the construction that we have described only involves states with nearest-neighbour spin correlations, a linear superposition of such states can involve valence bonds of any length. The five extra hops lead to spin configurations with longer range singlets, but the new states have non-zero overlaps with the original basis and hence can contribute directly to the energy of our starting wavefunction.

A critical observation is that it is *impossible* not to avoid some triplet character and therefore impossible not to lose some Kondo energy. An electron cannot be in a spin singlet with *both* of its nearest-neighbouring cerium atoms simultaneously. The trick is to ensure that it only delocalizes *into* Kondo singlets.

In order to try to understand the role of the five extra hops, it is convenient to take the states in our nearest-neighbour basis in pairs. The pairs of relevant states are those which are connected together by the seventh hop, where the charge carrier ends up being in a spin singlet with a different special atom. An application of the Hamiltonian to these pairs is depicted in figure 8. It is helpful to analyse the relationship between the spin correlations and the relative phase of our initial states: clearly the electron is in a spin singlet with one nearest-neighbour cerium atom and can gain Kondo energy from delocalizing about that atom, but what about the other cerium atom? If the electron is in a relative triplet, then it is non-bonding and cannot delocalize. If the electron is in a relative singlet, then it is bonding and delocalizes into a Kondo singlet. This is *precisely* the content of figure 8. The final contributions are cancelling contributions which can be attributed to the situations where the charge carrier is in a spin triplet with the other neighbouring spin. The non-orthogonality complicates this picture badly since there is even an overlap between the two pictured contributions! Note, however, that if the breakdown of the hopping energy includes the seventh hop in this contribution, then the final term disappears and we are left with the pure Kondo singlet combined with the longer range singlet combinations.

Let us focus on the first case where the charge carrier hops through an angle of 60°. The states that result are elements of the original basis. Further, the phase is such that these contributions add constructively, decreasing the hopping energy. This is the resonant superposition alluded to in section 2. Since we are considering a pair of original states, there is a maximal addition of *two* new hops for each state which yields a lower bound of $-9X$ for the ground-state energy. This bound is a *rigorous* bound, and can be proven by showing that the maximum simultaneous probability that

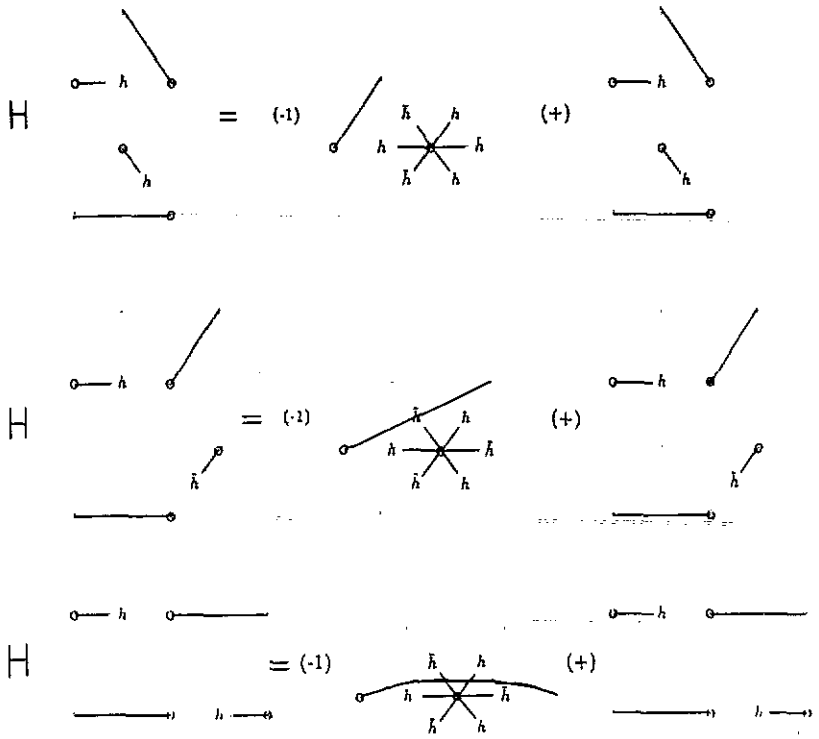

Figure 8. A diagrammatic representation for the five hops not included directly in an application of the Hamiltonian to our interpretational wavefunction for the triangular lattice. The charge carrier is denoted by h, a singlet configuration is denoted by a line with an encircled end, and a bar denotes the opposite sign to the contribution.

the spin on an electron is in a singlet with *both* of its neighbours is three-quarters each. Coherent motion for *all* singlet configurations yields $\frac{3}{4} \times (-12X) = -9X$, and all triplet contributions must be non-bonding and contributing nothing. This bound is achieved for the three atom per unit cell periodic boundary conditions calculation, but it is reduced to about $-8X$ for the infinite system when the 120° and 180° contributions are required. The role of the extra hops for pairs at 120° and 180°, is analogous to that for quantum fluctuations in the Néel description of quantum antiferromagnetism; they distort the picture locally leading to a 'softening' of the picture but they achieve a corresponding gain in hybridization energy.

There are *two* important ways that the extra hops contribute. First, the states depicted in figure 8 are not orthogonal to our starting state and hence contribute directly to the energy. For the first time there is a *cancellation* which reduces the ground-state energy. The hop where the charge carrier remains immobile contributes a loss of $X/2$ which corresponds to the ratio of probabilities that there is a triplet or singlet spin configuration; three-quarters of the time the charge carrier is in a triplet with the exchanged spin yielding $3X/4$ and one-quarter of the time they are in a singlet yielding $-X/4$. There are also smaller overlaps with the other states in our original interpretational wavefunction which further complicate the picture and these will be examined later. Second, the hybridization into the states depicted in figure 8 will induce a higher probability of finding them and a corresponding gain in hopping energy.

It must be borne in mind that the contributions from both 60° hops and non-orthogonality will lead to a preference of some spin configurations over others, and this will destroy the assumption that we want an *equal* superposition of states with nearest-neighbour singlets. Our interpretation of the spin correlations in section 3 suggests that the preference for 60° hops is a strong effect and leads to the enhanced probability for the charge carrier to reside on a triangle with two special atoms in a total spin singlet. On the other hand, the inclusion of the states depicted in figure 8 promotes triplet correlations for the two spins which neighbour the charge carrier, and this triplet character is strong, which suggests that this hybridization is also relevant. In the numerical calculations, we did observe that the lower the total spin of the state, the weaker the triplet character of this bond. Most of the triplet character can be explained by the spin configurations with the charge carrier on a triangle with a pair of special atoms in a spin singlet, since for these cases the bond is expected to be fully triplet. The residual triplet character might also be explainable in terms of correlations induced by the particular superposition imposed in our interpretational wavefunction, a point which remains unclear.

One of the weaker effects so far discussed is the non-orthogonality between the new states depicted in figure 8 and the states in our interpretational wavefunction. If we ignore the superposition complication, then for the largest overlaps we find overlap matrix elements of size $(-1)^n 2^{1-n} X$, where n is the number of non-identical singlets in a comparison between the two states. When $n = 2$ we find $X/2$ which is the cancellation previously mentioned resulting from the high probability that the charge carrier is in a spin triplet with one of its nearest-neighbour spins. This contribution is included in our discussion of 60° hops and reduced the bound on the hopping energy to $-9X$. Indeed for these contributions the triplet-spin configurations exactly cancel out leaving only the singlet hops which are all completely in phase with each other. The contribution from 120° and 180° hops is a penalty not so far included, but this contribution is reduced when the states of figure 8 are allowed to appear in the ground state. The next strongest contribution yields matrix elements $-X/4$ and decreases the ground-state energy. The overall contribution from this source is difficult to quantify, but we feel that it is probably small.

The interpretational wavefunction that we have presented probably has a variational energy around $-7X$. Figure 8 gives a very precise description of the effects neglected, and one might then ask why these effects are not then included variationally, resulting in a test of how good the description is. The reason is elementary but crucial; the non-orthogonality is such an extreme complication that including any new state variationally is beyond the technical expertise of the author. Even evaluating the overlap between the states in figure 8 is too difficult.

Although an analytic treatment of our interpretational wavefunction appears too difficult, one might expect to be able to test the wavefunction on the clusters used in our numerical work. Even this analysis appears to be too difficult due to a mixture of combinatorics and the requirement that the relative phase of the contributions is chosen correctly. However there is a numerical calculation that we can perform to achieve some insight. The relative phase of contributions is easy to find along a path that the charge carrier traces out. We have constructed states by taking an equal superposition of periodic nearest-neighbour paired states which correspond to a prescribed path, combined with an average over all six positions of the charge carrier around the special site with which it is in a relative singlet. A single state achieves an energy of $\sim -5.5X$, and a random path achieves an energy of ~ -6.5–$7.0X$. If

we further choose a path that favours 60° hops, we can easily achieve an energy of $\sim -7.4X$, which is over 90% of the ground-state energy. The spin correlations of such a state are very similar to those of the ground state, with the major differences being a higher probability of finding the charge carrier on one of the three conduction atom sublattices, attributable to a biased path, and slightly higher nearest-neighbour singlet correlations, as might be expected. Partially optimizing the energy in the singlet subspace where all nearest neighbours are paired, leads to the ground state itself or to a state with an energy only 2% above the ground state energy for our small clusters.

The interpretation of this section seems restricted to being a pictorial aid rather than a calculational procedure. Even the long-range characteristics of the spin correlations remain questionable. The energy associated with long-range order in this type of model is very small, and our interpretational wavefunction without any long-range correlations may well achieve long-range order when the 'quantum fluctuations' are included. The analogous situations for the Heisenberg model indicate that long-range aspects are immensely difficult to discover without an exact solution.

Perhaps the most difficult point to understand is why we believe that the physics is described by our variational wavefunction. At first sight, the 120° and 180° hops depicted in figure 8 yield states with Kondo singlets which could play an important role in the ground state. The critical point is that much of their content is *already included* and the orthogonal contribution is at higher energy involving more energetically unfavourable triplet correlations. This can be rigorously proven for the linear chain geometry [16], where the Heisenberg ground state controls the physics and the first orthogonal states, which are analogous to the new spin configurations here, are at least $+4X$ higher in energy.

Before we move on to the more difficult corresponding analysis for the square lattice, we would like to analyse the behaviour of the state corresponding to Nagaoka's [12] solution to one charge carrier moving in a strong-coupling Hubbard model; the single-bound-magnon problem.

This problem arises quite naturally in the X–J model. When the tight binding model for perovskite superconductors was first being analysed, there was a claim that the strong-coupling limit was identical to that for the square lattice Hubbard model. The justification was that an added hole would prefer to form a local singlet configuration with its neighbouring copper spin. The resulting object would be stable at low energies and would then move around the lattice in an analogous way to a vacant site in the strong-coupling Hubbard model. Nagaoka showed that in the absence of Heisenberg interactions a single hole moving under the action of the strong-coupling Hubbard model drives the spin background into a saturated ferromagnet [12]. For the X–J model an added hole does want to form a local singlet configuration and so it is quite natural to study the motion of this singlet under the action of the X-model. If the assumption that the strong-coupling Hubbard model were equivalent to the X–J model is correct, then we would expect Nagaoka's result to apply. In fact we discover *exactly the opposite results to Nagaoka.*

Nagaoka suggested ferromagnetism for bipartite lattices and *not* ferromagnetism for non-bipartite lattices with positive hopping matrix elements. We find ferromagnetism where paramagnetism is predicted and paramagnetism where ferromagnetism is predicted. To demonstrate these results we have solved the problem of one hole which has captured one magnon (or spin-flip) moving around in an otherwise ferromagnetic background.

There are two ways to do the calculation. First one can note that the magnon is tightly bound to the charge carrier and perform a variational calculation for states with increasing magnon–charge carrier separation. Secondly, one can evaluate the Green's function for the case of saturated ferromagnetism and use it, in combination with an impurity calculation to describe the states where the magnon is involved, to evaluate an exact expression for the energy. The resulting closed form solutions are:

$$G(\epsilon) = \int_0^1 \frac{(-\epsilon)\,dx}{\sqrt{[6-\epsilon\mp 3\pm(2c-1)^2]}\sqrt{[6-\epsilon\mp 3\pm(2c+1)^2]}} - 1$$
$$= \left[\frac{6(1\pm\gamma)}{\epsilon} - 1\right]^{-1} \tag{3}$$

for the triangular lattice with periodic (top sign) and antiperiodic (bottom sign) boundary conditions around a triangle, where $c = \cos(\pi x)$ and γ is the normalized structure factor for the triangular lattice. The resulting dispersions are depicted in figure 9. The numerical results indicate that periodic boundary conditions around a triangle yield the single-bound-magnon state as the ground state, but that antiperiodic boundary conditions around a triangle yields paramagnetism by at least an energy of X. The corresponding calculation for the square lattice has been published in a previous article [2]. The closed form solution being

$$G(\epsilon) = \int_0^1 \frac{(-\epsilon)\,dx}{\sqrt{[6-\epsilon+2c]}\sqrt{[2-\epsilon+2c]}} - 1 = \left[\frac{4(1+\gamma)}{\epsilon} - 1\right]^{-1}. \tag{4}$$

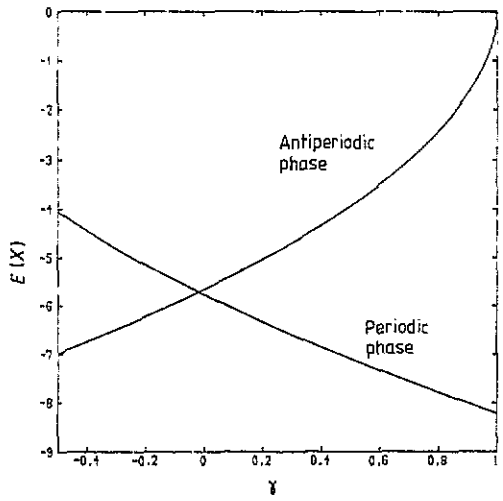

Figure 9. The dispersion relationship for the single-bound-magnon problem. The vertical and horizontal axes are energy (in units of X) and the triangular lattice structure factor, respectively. The curve which corresponds to periodic boundary conditions around a triangle yields a ground state at the zone centre, but the curve which corresponds to antiperiodic boundary conditions is about X above the true ground state of the system which is paramagnetic.

We now move on to an analytic interpretation for the square lattice. The basic idea is identical to that for the triangular lattice, but the bipartite nature of the square lattice presents severe complications. Our interpretational wavefunction is constructed by pairing up the charge carrier and one of its nearest neighbours into

a singlet together with all the other spins in nearest-neighbour singlet pairs. The charge carrier is then allowed to move by single hops to other states where all the spins are in nearest-neighbour singlets. The interpretational wavefunction is an equal superposition of all such connected spin configurations with the relative phase chosen so that all hops have negative phase. This choice ensures that five of the hops are in phase suggesting an estimate of $-5X$, together with three extra hops which conspire to provide the final half a hop.

So far the analysis is analogous to the triangular lattice case, but the state constructed does have a crucial difference; not all configurations are connected by direct hops. In fact the charge carrier is only ever in a spin-singlet configuration with spins on one of the two sublattices. The effect of the three extra hops is depicted in figure 10. As well as the cancelling contribution arising from the nearest-neighbour triplet configurations, we find states with the charge carrier in a singlet with a spin on the other sublattice. There is no possibility of finding the resonant contributions which so strongly stabilized paramagnetism on the triangular lattice. This lack can be traced to the fact that there are no odd loops in a bipartite lattice.

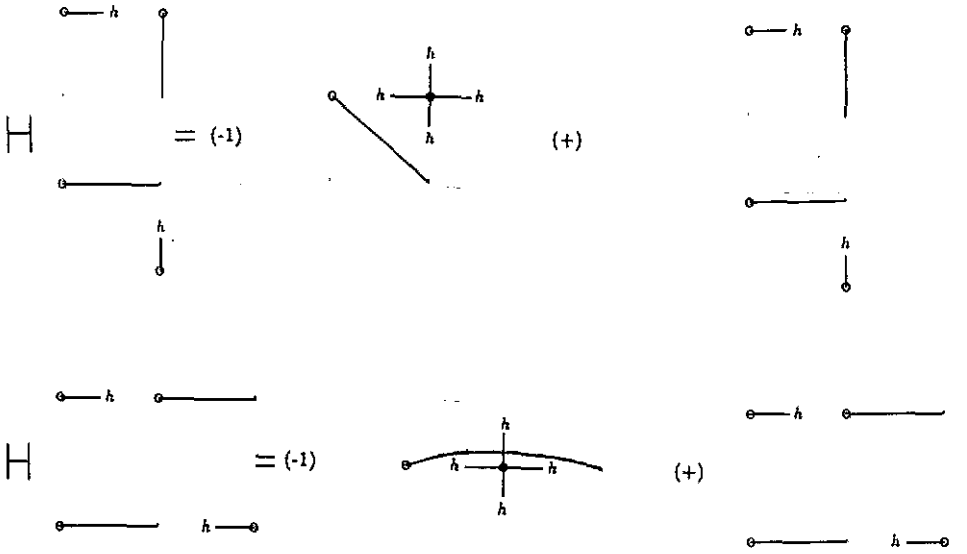

Figure 10. A diagrammatic representation for the three hops not included directly in an application of the Hamiltonian to our interpretational wavefunction for the square lattice. The symbols are the same as in figure 8.

One comparison which highlights the difference is the stability of paramagnetism over ferromagnetism. Comparing our numerical results with the single-bound-magnon problem, we find that paramagnetism is stable by about X for the triangular lattice but only by about $X/5$ for the square lattice. Our interpretational wavefunction is a much better description for the triangular lattice where the effects are stronger.

There are *two* of our interpretational wavefunctions for the square lattice and the extra hops act in a sense as a coupling between them. Variationally there is never a coupling between them, but the extra hops lead to a coupling for the true ground state. One way to measure how strong this coupling is, is to observe that the two spins which neighbour the charge carrier are decorrelated for our states. The extent to which this pair becomes triplet measures the distortion from mixing. In our

simulations this pair is fairly triplet but not as strongly triplet as for the triangular lattice.

6. Conclusions

Although the application of the X–J model to the perovskite superconductors is straightforward, the relevance to heavy fermions is not so clear. The processes which delocalize the conduction electrons are almost certainly stronger than the energy scale, X, which promotes the behaviour described in this article. There are several possible explanations: first the model may not apply and the dominant process is the conduction-electron delocalization. The only argument against this scenario is to ask why a simple RKKY-induced magnetism does not then result? Second it may be that fortuitously the delocalization processes 'cancel out' leaving the X–J model dominant. We do not believe this. Third, there is a type of renormalization argument. If we only elect to use electrons quite close to the Fermi surface, then the energy scale, X, can dominate and we might be led into the regime where the model applies. Since we only require a few electrons to dominate many spins for this model, this argument may not be too gross, since it does avoid the Nozières paradox [15]. Fourth, there is a very important new consideration that applies when a significant concentration of charge carriers are considered. We will look at this consideration in some detail.

The behaviour of many charge carriers in this model is usually more boson-like than fermion-like. The resulting avoidance of Pauli exclusion could then explain the stability and a condensation argument might also explain the superconductivity. The basic reasoning has been explained elsewhere [16] and we will only provide some intuitive explanation here. There is clearly only one type of charge carrier involved in our triangular lattice description. Further, this charge carrier has no spin degree of freedom associated with it. When two such charge carriers come together, they can actually sit on the same site, in a relative singlet. There is, however, a minor 'hard core' repulsion from the unavoidable probability that they are in a relative triplet. The particles cannot be considered as non-interacting, only as weakly interacting. The boson-like characteristics are found when two charge carriers are exchanged. If the charge carrier is always in a relative singlet with a nearest neighbour, then the exchange of two charge carriers involves an exchange of the two relevant singlets, and each singlet involves two particles. *Two fermions make a boson* and so if the exchange is made without breaking a singlet, exchange is bosonic in character. Another way to understand the result is to observe that, although the charge carrier is mobile, the underlying spins on the lattice do not move appreciably. When two charge carriers are exchanged, there is no corresponding exchange of electrons, and so no corresponding statistics requirement. A mathematical demonstration of this idea can be derived for the states developed in section 5 [16].

If the relevant electrons make use of the delocalization processes, then they retain their spin degree of freedom and meet as fermions. Fermi statistics ensures strong dispersion and some electrons fare better than others. If the electrons move via the X-model, then subject to a weak 'hard core' repulsion they can independently gain the full delocalization energy from their X-model motion. The low-spin state described in this article is strongly stabilized by an increasing concentration of charge carriers. This interpretation is certainly consistent with the behaviour of the perovskite superconductors.

In this article we have shown that, provided the smallest loop is not a triangle with periodic boundary conditions, then the X-model promotes a form of strong-coupling paramagnetism. A charge carrier dominates about five to ten special atom spins in its vicinity with the more distant spins readily distorted at a small cost in hopping energy. The spin correlations may be understood in terms of a linear superposition of states with only short-range singlets; a resonating valence bond state. The spin correlations appear to be much shorter range than in similar Heisenberg models.

Although it has previously been suggested that this model exhibits the same behaviour as the t–J model [1], as far as the charge motion is concerned we find *opposite* behaviour; where the t-model promotes ferromagnetism the X-model promotes paramagnetism and *vice versa*.

For the future, the next crucial feature which requires investigation is the coherence between charge carriers, and whether or not their behaviour is best represented by Bose statistics.

References

[1] Rice T M 1989 On the validity of the t–J model *Preprint*
[2] Long M W 1990 *J. Phys.: Condens. Matter* **2** 3829; 1989 *J. Phys.: Condens. Matter* **1** 9421
[3] Stewart G R 1984 *Rev. Mod. Phys.* **56** 755
[4] Steglich F, Aarts J, Bredl C D, Lieke W, Meschede D, Franz W and Schafer H 1979 *Phys. Rev. Lett.* **43** 1892
[5] Varma C M 1976 *Rev. Mod. Phys.* **48** 219
[6] Fehrenbacher R and Long M W 1989 unpublished
[7] Long M W and Barford W *RAL-89-053 and RAL-89-054*
[8] Anderson P W 1987 *Science* **235** 1196
Faddeev L D and Takhtajan L A 1981 *Phys. Lett.* **85A** 375
[9] Long M W 1989 *Z. Phys.* B **77** 47
[10] Murani A P, Knorr K, Buschow K H J, Benoit A and Floquet J 1980 *Solid State Commun.* **36** 523
[11] Zhang F C and Rice T M 1988 *Phys. Rev.* B **147** 3759
[12] Nagaoka Y 1966 *Phys. Rev.* **147** 392
[13] Long M W and Fehrenbacher R 1990 *J. Phys.: Condens. Matter* **2** 2787; unpublished
[14] Long M W 1988 *Z Phys.* B **69** 409
[15] Nozieres P 1985 *Ann. Phys., Paris* **10** 19
[16] Long M W unpublished